Sec3-containing Exocyst Complex Is Required for Desmosome Assembly in Mammalian Epithelial Cells

Nicholas J. Andersen* and Charles Yeaman*†

†Department of Anatomy and Cell Biology and *Program in Molecular and Cellular Biology, Carver College of Medicine, University of Iowa, Iowa City, IA 52242

The Exocyst is a conserved multisubunit complex involved in the docking of post-Golgi transport vesicles to sites of membrane remodeling during cellular processes such as polarization, migration, and division. In mammalian epithelial cells, Exocyst complexes are recruited to nascent sites of cell–cell contact in response to E-cadherin–mediated adhesive interactions, and this event is an important early step in the assembly of intercellular junctions. Sec3 has been hypothesized to function as a spatial landmark for the development of polarity in budding yeast, but its role in epithelial cells has not been investigated. Here, we provide evidence in support of a function for a Sec3-containing Exocyst complex in the assembly or maintenance of desmosomes, adhesive junctions that link intermediate filament networks to sites of strong intercellular adhesion. We show that Sec3 associates with a subset of Exocyst complexes that are enriched at desmosomes. Moreover, we found that membrane recruitment of Sec3 is dependent on cadherin-mediated adhesion but occurs later than that of the known Exocyst components Sec6 and Sec8 that are recruited to adherens junctions. RNA interference-mediated suppression of Sec3 expression led to specific impairment of both the morphology and function of desmosomes, without noticeable effect on adherens junctions. These results suggest that two different exocyst complexes may function in basal–lateral membrane trafficking and will enable us to better understand how exocytosis is spatially organized during development of epithelial plasma membrane domains.

INTRODUCTION

Protein complexes involved in membrane trafficking are structurally conserved from yeast to mammals. One such complex is the hetero-octameric Exocyst complex, which comprises Sec3, Sec5, Sec6, Sec8, Sec10, Sec15, Exo70, and Exo84 (Hsu *et al.*, 1996; TerBush *et al.*, 1996). Exocyst complexes are enriched at sites of active membrane expansion and are hypothesized to function as molecular tethers that anchor transport vesicles to the plasma membrane before soluble *N*-ethylmaleimide-sensitive factor attachment protein receptor-mediated fusion. In budding yeast, the Exocyst is recruited to presumptive bud sites and the tips of small-budded cells during early apical growth and to the mother-bud neck during cytokinesis (TerBush and Novick, 1995; Finger *et al.*, 1998). In plants, this complex accumulates at the apex of growing tobacco pollen tubes and is required for cellular morphogenesis (Hala *et al.*, 2008). In mammals, it is enriched at sites of membrane remodeling, such as neuronal growth cones (Hazuka *et al.*, 1999), podocyte foot processes (Simons *et al.*, 1999), the leading edges of migrating cells (Rosse *et al.*, 2006; Zuo *et al.*, 2006; Spiczka and Yeaman, 2008) and apical junctional complexes (AJCs), which include adherens junctions and tight junctions, of expanding lateral membranes such as those of polarizing epithelial Madin-Darby canine kidney (MDCK) cells (Yeaman *et al.*, 2004).

Address correspondence to: Charles Yeaman (charles-yeaman@uiowa.edu).

Abbreviations used: Dsc, desmocollin; Dsg, desmoglein.

The earliest studies of Exocyst function in polarized epithelial cells showed it to be required for basal–lateral delivery of newly synthesized low-density lipoprotein receptors but not for apical delivery of p75 neurotrophin receptors (Grindstaff *et al.*, 1998). Subsequent studies showed that additional pools of Exocyst complexes localized to and functioned within the endocytic system (Folsch *et al.*, 2003; Langevin *et al.*, 2005; Oztan *et al.*, 2007), endoplasmic reticulum (ER) (Lipschutz *et al.*, 2003), primary cilia/basal bodies (Rogers *et al.*, 2004; Park *et al.*, 2008; Overgaard *et al.*, 2009; Zuo *et al.*, 2009), and apical plasma membrane (Shin *et al.*, 2000; Beronja *et al.*, 2005; Blankenship *et al.*, 2007) of certain polarized epithelial cell types. In addition, an essential role for the Exocyst at the cleavage furrow and midbody of dividing cells has been described previously (Fielding *et al.*, 2005; Gromley *et al.*, 2005; Cascone *et al.*, 2008). Although it is clear that Exocyst activities are required for efficient membrane delivery to multiple destinations within the exocytic and endocytic systems, it is not known whether the same Exocyst holocomplex mediates each of these trafficking events, or whether distinct Exocyst complexes specify disparate tethering events at different target membranes.

Of the eight Exocyst subunits, Sec3 is exceptional in many respects. Under certain conditions, the budding yeast orthologue Sec3 is nonessential for growth and secretion (Finger and Novick, 1997; Wiederkehr *et al.*, 2004). However, cells lacking Sec3 have polarity defects. Indeed, Sec3 was hypothesized to be a spatial landmark for sites of polarized secretion because Sec3-green fluorescent protein (GFP) fusion proteins localized to presumptive bud sites even in the face of disruption of the actin cytoskeleton, secretion, and the function of other Exocyst subunits (Finger *et al.*, 1998). In photobleaching recovery experiments, Sec3 was the only Exocyst component that was not, at least in part, delivered to

secretion sites on transport vesicles (Boyd *et al.*, 2004). Although the polarized localization of Sec3 in budding yeast was insensitive to blocks in membrane traffic and disruption of the actin cytoskeleton, it depended on direct interactions with active Rho1 and Cdc42 GTPases (Guo *et al.*, 2001; Zhang *et al.*, 2001). Sec3 associates with plasma membranes directly by binding phosphatidylinositol 4,5-bisphosphate (Zhang *et al.*, 2008), a property that is shared with the Exo70 subunit (He *et al.*, 2007; Liu *et al.*, 2007). Finally, *sec3* mutants are unique among yeast Exocyst mutants because they display an aberrant ER distribution (Finger and Novick, 1997). Sec3 was recently shown to be required for inheritance of the cortical ER during yeast cell division, and its role there may be to stabilize associations between the ER tubules and the bud as they are delivered to it (Wiederkehr *et al.*, 2004). Collectively, these results show that Sec3 is an important and potentially multifunctional protein in budding yeast, with roles in both cell polarity and organelle inheritance.

In contrast to yeast Sec3, very little is currently known about its mammalian orthologue, which is the last subunit of the mammalian Exocyst complex to have been identified (Brymora *et al.*, 2001; Matern *et al.*, 2001). Unlike yeast Sec3, the mammalian protein lacks an amino-terminal Rho binding domain, so it is unlikely to directly bind GTPases of the Rho family (Matern *et al.*, 2001). Nevertheless, Sec3 interacts with the polarity protein IQGAP1 to facilitate the targeted delivery of matrix metalloproteinases to tumor cell invadopodia, and this interaction seems to be regulated by the RhoA and Cdc42 GTPases (Sakurai-Yageta *et al.*, 2008). It is possible that in metazoans accessory proteins link Sec3 to Rho GTPases. In fact, ICR1, a tropomyosin-related protein, was recently suggested to serve this function in *Arabidopsis* (Lavy *et al.*, 2007). A GFP fusion of human Sec3 failed to assemble into Exocyst holocomplexes and remained cytosolic when expressed in MDCK cells (Matern *et al.*, 2001) but was recruited to plasma membranes when coexpressed with GLYT1, a glycine transporter with which Sec3 interacted in vitro (Cubelos *et al.*, 2005). However, the localization and function of endogenous mammalian Sec3 have not been investigated. Because this subunit is important for ensuring correct polarized localization of Exocyst complexes in budding yeast, this represents an important gap in our knowledge of the mammalian Exocyst complex.

MATERIALS AND METHODS

Antibodies and Fluorescent Probes

Mouse monoclonal antibodies (mAbs) against Sec6 (9H5 and 8A5) and Sec8 (2E9, 2E12, 5C3, 7E8, 8F12, 10C2, and 17A10), and rabbit polyclonal antibodies against Sec3CT, Sec15, Exo70, and Exo84 have been described previously (Hsu *et al.*, 1996; Kee *et al.*, 1997; Yeaman, 2003). Rabbit polyclonal antibodies against Sec3NT were generated by immunizing rabbits with a His$_6$/V5-tagged fragment of human Sec3 (residues 2-205) that was expressed in bacteria and purified by binding to Talon beads (Clontech, Mountain View, CA) and eluted with imidazole (Fluka Biochemika, Buchs, Switzerland), according to manufacturer's instructions. Rabbit polyclonal antibodies against E-cadherin (E2 and UVO) and α-catenin have been described previously (Marrs *et al.*, 1993; Hinck *et al.*, 1994). A mAb against the extracellular domain of E-cadherin from MDCK cells (3G8) was the generous gift of Dr. Warren Gallin (University of Alberta, Edmonton, AB, Canada) (Wollner *et al.*, 1992). Chicken anti-pericentrin B/kendrin antibody was obtained from Dr. Trisha Davis (University of Washington, Seattle, WA) (Flory *et al.*, 2000). Pan-specific rabbit polyclonal antibodies to desmoglein (ab14417; AbCam, Cambridge, MA) and desmoplakin-1/2 (ab14418; AbCam), and mouse mAbs to β-tubulin (TUB 2.1; Sigma-Aldrich, St. Louis, MO) and γ-tubulin (GTU-88; Sigma-Aldrich) were obtained from commercial sources. Polyclonal chicken anti-plakoglobin antibody (1407) (Gaudry *et al.*, 2001); mouse mAbs to desmoglein 1 (Dsg1) (4B2) (Getsios *et al.*, 2004), desmoglein 2 (Dsg2) (6D8) (Wahl, 2002), and desmocollin-2/3 (Dsc2/3) (7G6) (Wahl *et al.*, 1996); and a retroviral vector encoding a Dsg2-FLAG-GFP chimera (Klessner *et al.*, 2009) were generously provided by Dr. Kathleen Green (Northwestern University Feinberg School of

Medicine, Chicago, IL). Fluorescein isothiocyanate (FITC)-goat anti-mouse, Texas Red-donkey anti-mouse, and Texas Red-donkey anti-rabbit immunoglobulin (Ig)G were purchased from Jackson ImmunoResearch Laboratories (West Grove, PA). Alexa594-goat anti-chicken IgY was purchased from Invitrogen (Carlsbad, CA). Horseradish peroxidase-conjugated rabbit anti-chicken IgY was purchased from Promega (Madison, WI). ^{125}I-labeled goat anti-mouse IgG and ^{125}I-labeled goat anti-rabbit IgG were purchased from Perkin Elmer Life and Analytical Sciences (Boston, MA).

Cell Culture Methodology

MDCK strain II cells were maintained in low glucose (LG)-DMEM containing 1 g/l sodium bicarbonate and supplemented with 10% fetal bovine serum (FBS; Atlas Biologicals, Fort Collins, CO), penicillin, streptomycin, and gentamicin (PSG). Low-density, contact-naïve MDCK cells were generated as described previously (Grindstaff *et al.*, 1998) and plated on collagen-coated coverslips in LG-DMEM containing 5 μM Ca^{2+} (LCM) supplemented with 10% dialyzed FBS for 2 h. For calcium switch experiments, LCM was replaced with MDCK growth medium for various times, as indicated in the figures. MCF-10A and human bronchial epithelial cells (HBECs) were grown as described previously (Debnath *et al.*, 2003; Kizhatil and Bennett, 2004). HeLa and Caco-2 cells were grown in high-glucose DMEM supplemented with 10% FBS, PSG, minimal essential medium (MEM)-nonessential amino acids, and 1 mM sodium pyruvate. Mouse inner medullary collecting duct cells (IMCD-3) were grown in DMEM/F-12 supplemented with 10% FBS, PSG, MEM-nonessential amino acids, and 1 mM sodium pyruvate. Bovine brain cytosol (BBC) was isolated as described previously (Malhotra *et al.*, 1989).

To achieve knockdown of Sec3 expression in MCF-10A cells, pLKO.1 lentiviral vectors encoding short hairpin RNAs (shRNAs) targeting both splice variants of human Sec3 were obtained from Open Biosystems (www.openbiosystems.com). These shRNAs targeted nucleotides 1473-1493 (sense: 5′-CCTGTTGGATATGGGAAACAT-3′, hairpin 1) and 1244-1264 (sense: 5′-CCCGACTATATGAAAGAGAAA-3′, hairpin 2) of human Sec3 mRNA (NM_018261). The production of vesicular stomatitis virus G protein (VSVG)-pseudotyped lentiviral vectors in 293FT packaging cells followed established protocols (The RNAi Consortium, Broad Institute, MIT, Cambridge, MA). Stable knockdown of Sec3 was achieved by lentiviral infection of either adherent or suspended MCF-10A cells, followed by selection in 5 μg/ml puromycin. Control hairpin, also in a pLKO.1 lentiviral vector, was an shRNA targeting a sequence (sense: 5′-CCCAACGTCATCGAGTACTAT-3′) specific to murine Nek8 (NM_080849) obtained from Open Biosystems (Huntsville, AL; www.openbiosystems.com). A search of the human BLAST assembled genome revealed no significant similarities.

To achieve rescue, three wobble base mutations were inserted into hSec3 cDNA (A1348T, A1351T, T1354C), to render the expressed mRNA resistant to shRNA hairpin 2. Hairpin-resistant Sec3 (Sec3^{hr}) cDNA was ligated into pcDNA 3.1 and transfected into shSec3 MCF-10A cells by Amaxa nucleofection using solution T and program T20 (Lonza, Basel, Switzerland). For immunofluorescence experiments, cells were cotransfected with pcDNA 3.1-Sec3^{hr} and pmaxGFP (Lonza) at a 5:1 ratio to verify transfection efficiency, which was typically >90%.

Immunofluorescence Labeling

Cells were prepared for immunofluorescence by fixation in methanol at −20°C for 5 min or, alternatively, preextraction in 1% Triton X-100 in buffer containing 10 mM piperazine-*N,N′*-bis(2-ethanesulfonic acid), pH 6.8, 50 mM NaCl, 300 mM sucrose, and 3 mM MgCl$_2$ (CSK) before fixation in either methanol at −20°C for 5 min, or 4% paraformaldehyde at 4°C for 20 min. After cells were quenched in buffer containing 50 mM NH$_4$Cl, they were blocked in 0.2% fish-skin gelatin in Ringer's saline (10 mM HEPES, pH 7.4, 154 mM NaCl, 7.2 mM KCl, and 1.8 mM CaCl$_2$) for 20 min at room temperature. Antibodies were diluted in blocking buffer and applied to cells for 2 h at 4°C. After five washes in blocking buffer, FITC and Texas Red-conjugated secondary antibodies were applied for 1 h at 4°C. Coverslips were washed five times and mounted in VECTASHIELD containing 4,6-diamidino-2-phenylindole (Vector Laboratories, Burlingame, CA) or in Elvanol-PPD. Samples were viewed with either a Microphot-FX microscope (60× objective; Nikon, Tokyo, Japan) or a 510 laser scanning confocal microscope (63× objective; Carl Zeiss, Thornwood, NY), by using a krypton/argon laser with 488 nm (FITC) and 543 nm (Texas Red) laser lines, as noted in the figure legends. Digital images of data collected from the Microphot-FX microscope (Nikon) were obtained with a Kodak DCS 760 digital camera.

Hanging Drop Assay

Hanging drop assays were performed as described previously (Kim *et al.*, 2000). Cultures of parental and Sec3-knockdown MCF-10A cells were suspended by trypsin treatment, centrifuged, and resuspended at a concentration of 2.5 × 10^5 cells/ml. Fifty-microliter droplets were applied to the inside of a 10-cm tissue culture plate lid. Five milliliters of culture medium (Opti-MEM; Invitrogen) was added to the culture plate to prevent dehydration. After 20 h, lids were inverted and suspensions were either left untreated or triturated by pipetting twice with a 20-μl pipette tip that had been prewashed with phosphate-buffered saline (PBS) containing 0.1% Triton X-100 PBS, and rinsed with

PBS. Cell suspensions were then flattened with glass coverslips. Analysis of cell aggregates was performed by photographing several areas of each droplet using a TE300 microscope (Nikon) equipped with a Coolpix 5000 digital camera (Nikon). Cells were counted by determining area of aggregates normalized to the area of a single cell. The percentages of aggregates containing 1–2, 3–50, or 50+ cells were calculated.

Gel Electrophoresis and Immunoblotting

Protein samples were incubated in SDS-polyacrylamide gel electrophoresis (PAGE) sample buffer for 10 min at 65°C before separation in 7.5, 10, or 12.5% SDS polyacrylamide gels. Proteins were electrophoretically transferred from gels to Immobilon polyvinylidene difluoride (PVDF) membranes (Millipore, Billerica, MA). Blots were blocked in Blotto (5% nonfat dry milk, 0.5% normal goat serum, and 0.1% sodium azide in Tris-buffered saline [TBS]) overnight at 4°C. Primary antibodies were incubated with blots at room temperature for 1 h. After five washes, 10 min each, in TBS containing 0.1% Tween 20, the blots were incubated with ^{125}I-labeled goat anti-mouse or goat anti-rabbit secondary antibody for 1 h at room temperature. Blots were washed as described above and then twice in TBS and exposed to phosphorimager screens. The amount of labeled antibody bound to the blots was determined directly using a Phosphorimager (Typhoon; GE Healthcare, Little Chalfont, Buckinghamshire, United Kingdom) and ImageQuant software, version 5.0 (GE Healthcare).

Detergent Solubility Analysis

MDCK cells were washed three times with Ringer's saline on ice, and lysed in either CSK or radioimmunoprecipitation assay (RIPA) buffer (50 mM Tris-HCl, pH 7.5, 1% NP-40 0.25% sodium deoxycholate, 150 mM NaCl, and 1 mM EDTA) containing protease inhibitors (10 μg/ml each of pepstatin A, leupeptin, and antipain). Cell lysates were collected in 1.5-ml Eppendorf tubes and incubated on ice for 20 min. Detergent insoluble fractions were pelleted at 20,000 $\times$ g (Eppendorf 5417C) for 10 min at 4°C and extracted by repeated passage through 18-, 23-, and 25-gauge needles, in 1% SDS. Equal volumes of soluble and insoluble fractions were resolved by SDS-PAGE. Proteins were transferred to Immobilon P membranes for immunoblotting with antibodies specific for each Exocyst subunit, and signals were quantified with a phosphorimager, as described above.

Exocyst Fractionation

Cells were homogenized in isotonic sucrose buffer [0.25 M sucrose in 20 mM HEPES-KOH, pH 7.2, 90 mM KOAc, 2 mM Mg(OAc)$_2$, and protease inhibitors] by repeated passage through a ball bearing homogenizer (Varian Physics, Stanford University, Stanford, CA). Separation of different membrane compartments was achieved by centrifugation in three-step 10–20–30% (wt/vol) iodixanol gradients (Yeaman et al., 2001; Yeaman, 2003). One third of the postnuclear supernatant was mixed with Opti-Prep (60% [wt/vol] iodixanol; Nycomed, Oslo, Norway) and homogenization buffer to generate solutions containing 10, 20, or 30% iodixanol. Equal volumes of these solutions were layered in centrifuge tubes, and samples were centrifuged at 353,000 $\times$ g for 3 h at 4°C, in an NVt65 rotor (Beckman Coulter, Fullerton, CA). Fractions (0.5 ml) were collected, refractive indices were read, and proteins were separated by SDS-PAGE. Proteins were transferred from gels to Immobilon P membranes for immunoblotting, as described above.

For gel filtration analysis, confluent monolayers of MDCK cells were extracted for 10 min at 4°C, in Tris-saline buffer containing 0.5% (vol/vol) NP-40 and protease inhibitors. Cell lysates were centrifuged at 15,000 $\times$ g for 10 min. The supernatant fraction was centrifuged at 100,000 $\times$ g for 30 min and passed through a 0.22-μm syringe filter (Millipore). Then, 200 μl of this lysate was applied to a Superose 6 HR 10/30 column and fractionated as described previously (Stewart and Nelson, 1997). Fractions 6–28 were separated by SDS-PAGE, and proteins were electrophoretically transferred to Immobilon P membranes for immunoblotting with specific antibodies.

Immunoprecipitation

RIPA extracts of MDCK cells were pre-cleared with Pansorbin (Calbiochem, San Diego, CA) and incubated overnight with specific primary antibodies, prebound to protein A-Sepharose (GE Healthcare). Beads were pelleted by gentle centrifugation, and supernatant was transferred to fresh antibody-coupled beads. This was repeated for a total of three rounds (anti-Sec8—mAbs 2E12, 5C3, 10C2) or four rounds (anti-Sec3NT) of immunoprecipitations. Then, 10% of the starting extract and the final depleted supernatant were removed for analysis. For analysis of Exocyst complexes lacking Sec3, lysates depleted of Sec3 were subjected to immunoprecipitation with anti-Sec8 immunoadsorbant, overnight at 4°C. Samples were resolved by SDS-PAGE and immunoblotted with antibodies specific for Sec3, Sec6, and Sec8, after electrophoretic transfer to PVDF membranes as described above.

To determine relative expression levels of Sec3 and Sec8 in MDCK cells, cultures were metabolically labeled with [^{35}S]methionine/cysteine (EasyTag; PerkinElmer Life and Analytical Sciences) overnight, and amounts of each radiolabeled subunit were compared after immunoprecipitation with specific antibodies. To correct for immunoprecipitation efficiency differences, a non-

radioactive reference lysate was prepared, and recoveries of Sec3 and Sec8 were determined by quantitative immunoblotting with specific antibodies, as described above. This revealed that anti-Sec3 and anti-Sec8 immunoadsorbants recovered 53 and 93% of the Sec3 and Sec8 in the lysate, respectively. In addition, the relative masses of canine Sec3 (102,017 Da) and Sec8 (110,627 Da), as well as differences in methionine/cysteine content of the two proteins, were considered.

Surface Repopulation Assay

Control and Sec3 knockdown MCF-10A cells were seeded at confluent densities on 12-mm Transwell 0.45-μm polycarbonate filters (Corning Life Sciences, Lowell, MA) in LCM. At various time points after a calcium switch, cells were placed on ice and washed five times with Ringer's saline. Sulfo-NHS-SS-Biotin (Pierce Chemical, Rockford IL) (0.5 mg/ml in Ringer's saline) was applied to both apical and basal-lateral surfaces (0.5 ml apical/1 ml basal-lateral), and the cells were incubated twice for 20 min each, at 4°C, with gentle rocking. Biotinylation reactions were quenched by washing cells in five changes of TBS (120 mM NaCl and 10 mM Tris, pH 7.4) containing 50 mM NH$_4$Cl and 0.2% bovine serum albumin (quenching buffer), at 4°C. Cells were lysed in RIPA buffer containing 0.1% SDS and protease inhibitors at 4°C for 20 min, with gentle rocking. Lysates were centrifuged at 15,000 $\times$ g for 10 min, and supernatant fractions were transferred to clean tubes. Then, 10% of the lysate was removed and mixed with SDS-PAGE sample buffer for quantitation of total protein expression. The remaining lysate was combined with 50 μl of streptavidin-agarose (Pierce Chemical), incubated overnight at 4°C on a tube rotator, and then washed under stringent conditions (3 times in HS-buffer [0.1% SDS, 0.5% deoxycholate, 0.5% Triton X-100, 20 mM Tris-HCl, pH 7.5, 120 mM NaCl, 25 mM KCl, 5 mM EDTA, and 5 mM EGTA] and 3 times in low salt washing buffer [10 mM Tris-HCl, pH 7.5, and 2 mM EDTA]). Samples were resolved by SDS-PAGE, transferred to PVDF membranes, and probed with antibodies specific for Dsg2. Signals were quantified with a phosphorimager, as described above.

RESULTS

Sec3 Localizes to Desmosomes and Centrosomes

The localization of several endogenous Exocyst subunits in mammalian epithelial cells has been reported previously (Grindstaff et al., 1998; Lipschutz et al., 2000; Folsch et al., 2003; Prigent et al., 2003; Rogers et al., 2004; Oztan et al., 2007; Zuo et al., 2009) but that of Sec3 has yet to be examined. Although a Sec3-GFP fusion protein was shown to have a cytosolic distribution, it is unclear whether this reflects the localization of endogenous Sec3 (Matern et al., 2001). We approached this question by preparing polyclonal antibodies against fusion proteins representing either N- or C-terminal regions of human Sec3 (Figure 1A). Both antibodies were specific, as determined by a variety of criteria (Figure 1, B–G, and Supplemental Figure S1). Antibodies to both N- and C-terminal domains labeled pools of Sec3 distributed in a punctate, discontinuous pattern along the plasma membrane and in the cytoplasm of MDCK cells (Figure 1, E and F). Preimmune serum did not label either pool (Figure 1D), and immune serum depleted of Sec3-specific antibodies showed decreased levels of plasma membrane and cytoplasmic labeling (data not shown). Antibodies against the N terminus of Sec3 additionally labeled a perinuclear compartment in subconfluent MDCK cultures (Figure 1F). Therefore, in contrast to ectopic GFP-Sec3, endogenous Sec3 was, at least in part, associated with the plasma membrane and cytoplasmic organelles.

To determine whether Sec3 colocalized with other Exocyst subunits on lateral plasma membranes, we colabeled MDCK cells with anti-Sec3 C-terminal antibodies and monoclonal Sec6 and Sec8 antibodies. Specific Sec3 immunolabeling was coincident with that of Sec6 when one specific mAb (8A5), but not another (9H5), was used (Figure 2, A and B). In polarized MDCK cells, structures labeled by anti-Sec3 and anti-Sec6(8A5) were concentrated at two distinct sites along lateral membranes (Figure 2B). In contrast, anti-Sec3 antibodies did not label structures recognized by anti-Sec6(9H5) (Figure 2A), in spite of the fact that this antibody was pre-

Figure 1. Antibodies to Sec3 are specific. (A) Schematic representation of human Sec3. Three coiled-coil motifs (amino acids 152-176, 205-257, and 742-764) are predicted by the COILS program. Lines indicate regions of the protein that were used to generate antibodies. The N-terminal Sec3 (Sec3NT) peptide encompasses amino acids 2-205, and the C-terminal Sec3 (Sec3CT) peptide consists of amino acids 692-818. (B) The specificity of the anti-Sec3CT antibody was examined by Western blotting. A 100,000 × g postnuclear membrane pellet (p) and supernatant (s) were resolved by SDS-PAGE, and immunoblotted with Sec3CT preimmune serum, postimmune serum, and postimmune serum depleted of either glutathione transferase (GST) or GST-Sec3CT antibodies. Specific Sec3 signal was present only in the membrane fraction (p). (C) The specificity of the anti-Sec3NT antibodies was examined by Western blotting. 15 μg of RIPA lysates of MDCK, HBEC, Caco-2, IMCD-3, MCF-10A, and HeLa cells and also BBC, were resolved by SDS-PAGE and blotted against anti-Sec3NT preimmune, postimmune, and postimmune serum depleted of anti-GST-Sec3NT antibodies. In all cell lines and the BBC, a band corresponding to the predicted mass of Sec3 (102 kDa) was present. The smaller band present in some samples might represent a splice variant or be a consequence of protein degradation. (D and E) The specificity of anti-Sec3CT antibodies was examined by immunofluorescence. MDCK cells were fixed and labeled with anti-Sec3CT preimmune (D) or postimmune (E) serum. Anti-Sec3CT antibodies specifically labeled puncta on the plasma membranes and in the cytoplasm. (F) Anti-Sec3NT antibodies also labeled the plasma membranes in a punctate pattern but, in addition, labeled the perinuclear region. (G) 0.5 μg of the Sec3NT immunogen (Sec3NT-His/V5) was resolved by SDS-PAGE and immunoblotted with anti-Sec3NT and anti-V5 antibodies. Both the anti-V5 and anti-Sec3NT antibodies recognized the immunogen.
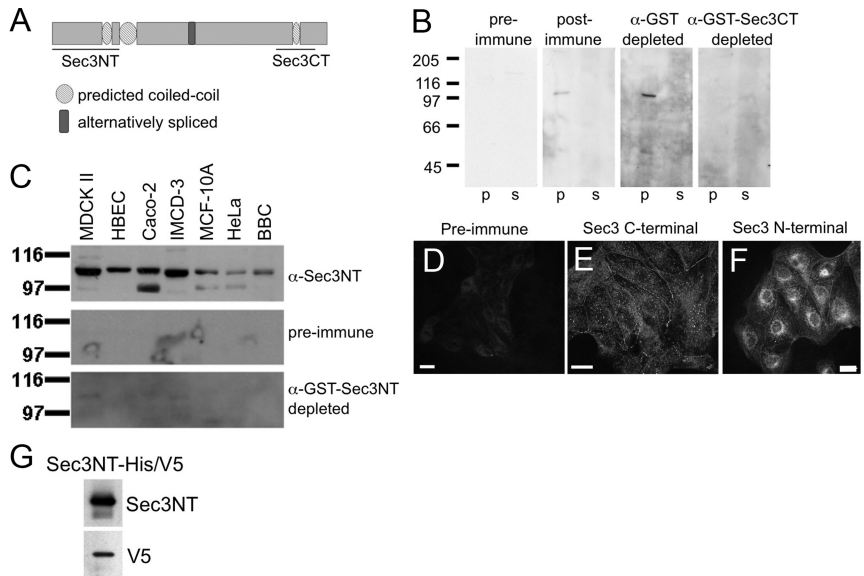
viously shown to label Exocyst pools associated with the AJC (Yeaman *et al.*, 2004). Sec3 localized to lateral membrane sites that were more basal than those detected by anti-Sec6(9H5). In addition, although the labeling pattern of anti-Sec6(9H5) was continuous and even, that of anti-Sec3 and anti-Sec6(8A5) was discontinuous and punctate. Therefore, although localization of Sec3 to lateral membranes was similar to that of other Exocyst subunits reported previously, Sec3 did not colocalize with previously characterized Sec6/8 complexes there.

To confirm that the novel punctate labeling pattern observed with anti-Sec3 and anti-Sec6(8A5) antibodies represented bona fide Exocyst localization, the distribution of several other Exocyst subunits was examined. Because prior studies of Sec8 localization in MDCK cells used a mAb (8F12) that did not colabel structures decorated by anti-Sec3 antibodies, we screened several fixation conditions and a panel of 10 mAbs to Sec8 to determine whether these proteins were colocalized in cells. We found that a cocktail of anti-Sec8 mAbs (2E9, 5C3, 7E8, and 17A10) applied to methanol-fixed cells labeled a pool of Sec8 that colocalized with Sec3 at the lateral plasma membrane (Figure 2C). Permeabilization of cells with Triton X-100 before fixation revealed that this Sec8 pool was, like Sec3, distributed in a punctate and discontinuous manner on the membrane (Supplemental Figure S2).

Polyclonal anti-Sec15 antibodies also labeled plasma membrane structures that were indistinguishable from those labeled by anti-Sec6(8A5) (Figure 2D). This labeling was enriched at sites of cell–cell contact and absent from free cell borders, consistent with Sec3 labeling at the plasma membrane. Furthermore, antibodies to Sec15 and two other Exocyst subunits, namely, Exo70 and Exo84, produced identical labeling patterns in A431 cells (Supplemental Figure S3). Thus, at least six different Exocyst subunits localized to similar punctate, lateral plasma membrane structures that

were distinct from the sites at which previously identified AJC-associated Sec6/8 complexes localized.

Because several Exocyst subunits were distributed in a characteristic spot-like pattern at sites of cell-cell contact, the possibility that these sites represented desmosomes was examined. Anti-Sec6(8A5) and anti-desmoplakin antibodies colabeled identical structures enriched in two regions of the lateral plasma membrane (Figure 2E). Moreover, Sec3 colocalized with desmoglein-GFP at these lateral membrane puncta (Figure 2F). These data show that Exocyst complexes containing Sec3 are enriched at desmosomes.

Not only this desmosome-associated Sec3 fraction but also an additional Sec3 pool was observed (Figures 2A and 3). Specifically, Sec3 colocalized with γ-tubulin (Figure 3A) and kendrin (pericentrin-B) (Figure 3B) at centrioles. Given that either one or two dots were conspicuous in polarized MDCK cells, Sec3 seems to associate with both maternal and daughter centrioles. In polarized cells, the majority of centrioles are located in the apical cytoplasm in a higher focal plane than desmosomes, so it is not surprising that not all optical sections showed both pools of Sec3 protein (Figure 3). Antibodies to Sec15, Exo70, and Exo84 also labeled centrosomes in A431 cells, suggesting that a Sec3-containing Exocyst complex is associated with this organelle (Supplemental Fig. S3).

Sec3 Occupies a Subset of Exocyst Complexes in Epithelial Cells

In contrast to published localizations of Sec6 and Sec8 at the AJC, Sec3 colocalized with Sec15, Exo70, and Exo84 and immunologically distinct pools of Sec6 and Sec8 at desmosomes. To determine whether distinct Exocyst complexes are associated with desmosomes and the AJC, we compared the biochemical properties of Sec3 and Sec8. First we examined the detergent solubility of each subunit. Sec3 solubility in buffer containing Triton X-100 was nearly identical to that of every other Exocyst subunit examined, except Exo84 (Figure
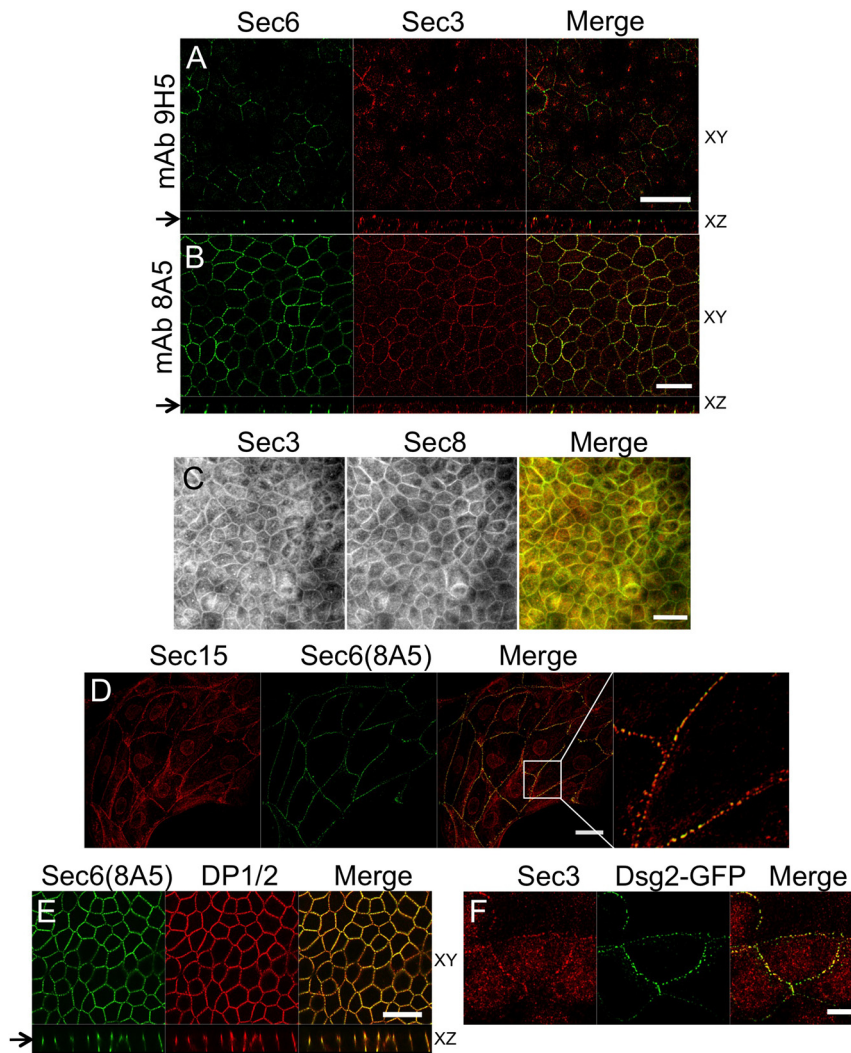
Figure 2. Exocyst localizes to desmosomes. (A) Polarized MDCK cells were colabeled with anti-Sec3CT and anti-Sec6(9H5) antibodies. Both en face (*xy*) and vertical (*xz*) confocal sections are shown, and the arrow denotes the position at which *xy* images were collected. The *xz* section demonstrates that endogenous Sec3 is enriched at sites on the lateral plasma membrane that are more basal than those labeled by anti-Sec6(9H5) antibodies. Bar, 20 μm. (B) Polarized MDCK cells were colabeled with anti-Sec3CT and anti-Sec6(8A5) antibodies. *xy* and *xz* confocal sections are shown. Note that Sec3 and Sec6 were colocalized at two distinct points of focal accumulation on lateral membranes. Bar, 20 μm. (C) Polarized MDCK cells were fixed in methanol and colabeled with anti-Sec3CT and a cocktail of anti-Sec8 mAbs (2E9, 5C3, 7E8, and 17A10). This method was required to visualize colocalization of Sec3 and Sec8 in polarized cells. Bar, 20 μm. (D) MDCK cells on collagen-coated coverslips were colabeled with anti-Sec15 and anti-Sec6(8A5) antibodies. Note that Sec15 and Sec6 were colocalized at puncta along contacting, but not noncontacting plasma membranes. The rightmost panel shows a magnified view of the boxed area in the panel to its left. Bar, 20 μm. (E) Polarized MDCK cells were colabeled with anti-Sec6(8A5) and anti-desmoplakin 1/2 (DP1/2) antibodies. *xy* and *xz* confocal sections are shown. Note that DP1/2 and Sec6(8A5) were colocalized at two sites on the lateral membrane. Bar, 20 μm. (F) MDCK cells seeded on collagen-coated coverslips were transduced with Dsg2-GFP adenovirus and labeled with anti-Sec3CT antibody. Endogenous Sec3 colocalized with Dsg2-GFP-positive puncta at the plasma membrane. Bar, 10 μm.

4 and Supplemental S4). Sec3 was, like Sec8, more soluble in deoxycholate-containing RIPA buffer (Figure 4). However, no significant differences in solubility were observed between Sec3 and Sec8, regardless of the solubilization buffer used.

Because the Exocyst associates with membranes, the buoyant densities of Sec3- and Sec8-associated membrane domains were analyzed by isopycnic density gradient centrifugation. Sec8 had been shown previously to cofractionate with proteins associated with the AJC—such as zona occludens (ZO)-1, ZO-2, nectin-2α, and E-cadherin—at $\delta = 1.16$ g/ml (Yeaman *et al.*, 2004). We found that membrane-associated Sec3 also cofractionated with Sec8 at $\delta = 1.16$ g/ml (Figure 5A). In addition, the desmosome-associated protein desmoplakin was enriched in these fractions, consistent with immunolocalization of Sec3 to desmosomes. A secondary peak of Sec3 and Sec8 corresponded to cytosolic fractions ($\delta = 1.20$ g/ml).

To determine whether Sec3 assembles into large, multimeric complexes similar in size to those containing Sec8, we fractionated detergent extracts of MDCK cells by Superose 6 fast-performance liquid chromatography. Most of the Sec3 coeluted with Sec8 in a single peak at fraction 12, corresponding to a protein complex with an apparent molecular size of >3000 kDa, based on the elution of globular protein standards (Figure 5B). In addition to this major peak, an overlapping peak of Sec8, centered at fraction 14 and corresponding to a protein complex of ~1000 kDa, was observed. Sec3 was not associated with this Sec8 fraction, but a minor pool of Sec3 was observed in fraction 19, as part of a protein complex of ~450 kDa. No Sec3 was recovered in fractions that eluted from the column at later time points, indicating that monomeric Sec3 was not present in detectable quantities in MDCK cells (data not shown). Instead, all of the Sec3 was assembled into high-molecular-weight complexes. In addition, these data hint that Sec8 may exist in at least two distinct complexes that either contain or lack Sec3.

To directly test this possibility, we performed coimmunoprecipitation studies. We performed three consecutive rounds of Sec8 immunoprecipitation in order to deplete this protein it from MDCK RIPA lysates (Figure 6A). Sec3 was almost completely cleared from the lysates after the first round of Sec8 immunoprecipitation, indicating that all of the Sec3 was associated with Sec8 in MDCK cells (Figure 6A). In contrast, exhaustive immunoprecipitation of Sec3 from the same lysates left ~30% of the Sec8 in the Sec3-depleted lysate (Figure 6B). Subsequent immunoprecipitation of this Sec8 pool also recovered Sec6 (Figure 6C). These results indicate that at least two distinct Sec8-containing Exocyst
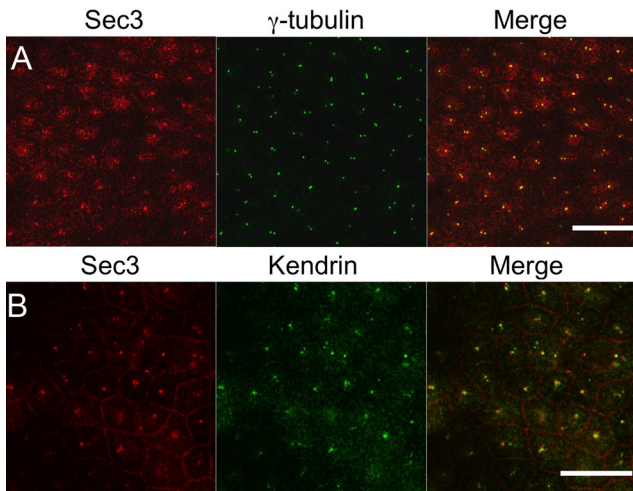
Figure 3. Sec3 localizes to centrioles. (A and B) Polarized MDCK cells were colabeled with anti-Sec3CT and either an anti-γ-tubulin (A) or an anti-kendrin (B) antibody. *xy* confocal sections are shown. Endogenous Sec3 was localized at kendrin- and γ-tubulin-positive structures. Bar, 20 μm.

complexes are present in MDCK cells, and that these are distinguished by the presence or absence of Sec3.

Assuming that all Sec3 and Sec8 were present in Exocyst complexes at a 1:1 stoichiometry, but additional Sec8-containing complexes lacking Sec3 were also present in cells, Sec8 should be more abundant than Sec3. To test this prediction, we immunoprecipitated Sec3 and Sec8 from radiolabeled cells (Figure 6D). After correcting for immunoprecipitation efficiencies and differences in the methionine and cysteine contents of the two proteins, we determined that MDCK cells had ~65% more Sec8 than Sec3.
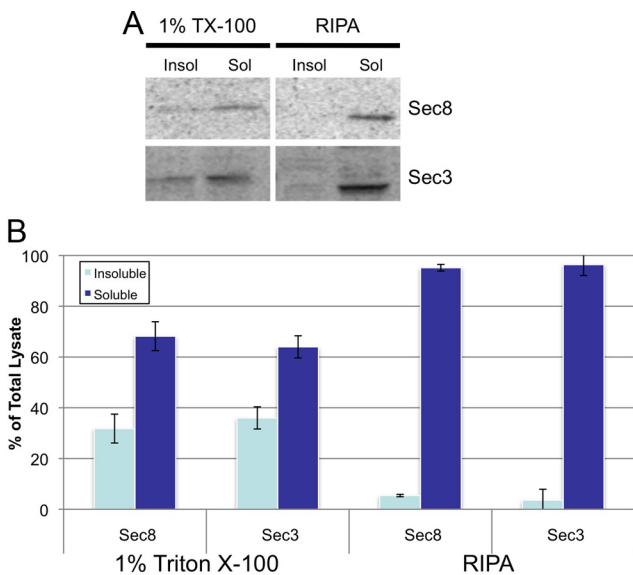

Figure 4. Sec3 and Sec8 have the same detergent solubility. (A) Insoluble (Insol) and soluble (Sol) MDCK fractions generated using 1% Triton X-100 or RIPA (deoxycholate) were analyzed by SDS-PAGE and immunoblotting with anti-Sec3NT and anti-Sec8(8F12) antibodies. (B) Quantitative analysis of data presented in A. Error bars represent standard deviations representing three independent experiments.
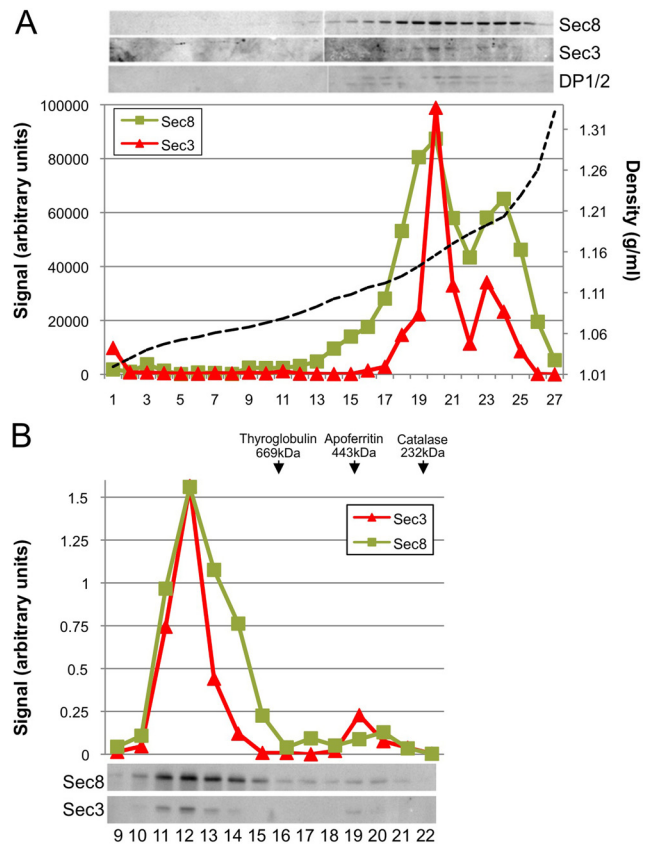

Figure 5. Sec3 and Sec8 cofractionate in an isopycnic density gradient and coelute on a gel filtration column. (A) MDCK postnuclear supernatants were fractionated on a 10–20-30% iodixanol step gradient. The density of each fraction was determined after measuring its refractive index (dotted line). Each sample was tested for the presence of Sec3, Sec8, and DP1/2, and the three proteins were found to cofractionate at a buoyant density of 1.16 g/ml. (B) Gel filtration chromatography by Superose6 FPLC. Fractions 9–22 were immunoblotted with anti-Sec3NT and anti-Sec8(8F12) antibodies. Molecular weight standards, 669 kDa, thyroglobulin; 443 kDa, apoferritin; and 232 kDa, catalase.

Finally, the spatiotemporal redistribution of Sec3 during early stages of cell–cell contact formation was compared with that of Sec6 and Sec8. The rationale for this experiment was that if distinct Exocyst complexes that either contain or lack Sec3 are associated with desmosomes and AJCs, respectively, it might be possible to observe differences in how they become associated with plasma membranes during polarity development. Contact-naïve MDCK cells were allowed to adhere to a collagen substrate at low plating density in LCM for 1 h, and then either maintained in LCM (Figure 7A) or switched to high calcium medium (HCM) for 1 h (Figure 7B). In cells cultured in LCM for 2 h, nascent E-cadherin–containing intercellular contacts formed, and these were labeled with anti-Sec6(9H5) and anti-Sec8(8F12), but not anti-Sec3 antibodies (Figure 7A). Although Sec3 was not present at these nascent cellular contacts in LCM, it did colocalize with Sec6, Sec8 and desmosomal cadherins in cytoplasmic puncta (Figure 7, A and C). Only after culturing cells in HCM for 1 h was Sec3 observed to accumulate at sites of intercellular contact (Figure 7B). Therefore, membrane recruitment of the Sec3 protein, which ultimately becomes associated with desmosomes, was slower than that of the Sec6/8 complexes that associate with the AJC.
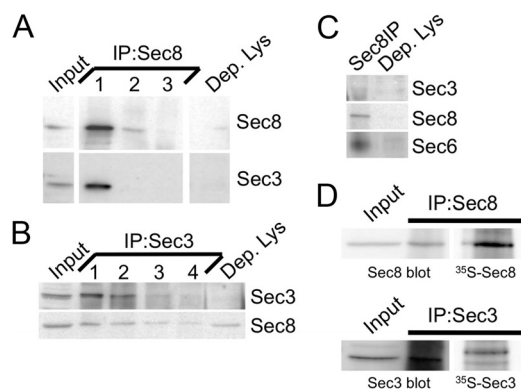
Figure 6. All endogenous Sec3 is bound to Sec8. (A and B) MDCK RIPA extracts were immunoprecipitated several times with anti-Sec8- (A) or anti-Sec3NT (B)-bound protein A-Sepharose. Input lysate (Input) represents 10% of starting material. Depleted lysate (Dep. Lys) represents 10% of the final post-immunoprecipitation supernatant. Samples were resolved by SDS-PAGE and immunoblotted with anti-Sec3NT and anti-Sec8(8F12) antibodies. Note that Sec3 was fully depleted by three rounds of Sec8, and four rounds of Sec3 immunoprecipitation, whereas Sec8 was still present in the Sec3-depleted lysate. (C) Sec8 was immunoprecipitated from the Sec3-depleted lysate. Sec8 immunoprecipitation and 10% of the final postprecipitation supernatant were immunoblotted with anti-Sec3, anti-Sec8(8F12), and anti-Sec6(9H5) antibodies. Note that Sec6 was associated with Sec8 in a complex that did not contain Sec3. (D) MDCK cells express more Sec8 than Sec3. Sec8 and Sec3 were immunoprecipitated from both nonlabeled and [^{35}S]methionine/cysteine-labeled MDCK cells. Relative expression levels of each protein were determined as described in *Materials and Methods*.

Sec3 Is Required for Desmosome Assembly

To study the role of Sec3 in epithelial cells, we reduced its expression in human MCF-10A cells by transduction with lentiviral vectors containing a puromycin selection cassette and shRNAs targeting both splice variants of human Sec3. It was necessary to switch to these cells because multiple efforts to stably reduce Sec3 to levels below ~50% of control levels in MDCK cells were unsuccessful. MCF-10A cells form a polarized, cuboidal epithelium with well-developed desmosomes and adherens junctions (Tait *et al.*, 1990). We identified two hairpins that reduced Sec3 protein levels by >90%, as assessed by Western blotting (Figure 8A). These also led to greatly reduced immunofluorescence labeling intensity after selection in puromycin (Figure 8B).

Because Sec3 accumulated at desmosomes, we determined whether it was required for the structural integrity of these junctions. Pan-specific desmoglein antibodies labeled spot-like desmosomes along plasma membranes of control cells, but this plaque-like labeling was disrupted in Sec3 knockdown cells. In these cells, most of the membrane-proximal desmoglein-positive structures were organized into linear arrays that ran perpendicular to cell–cell contacts (Figure 8, C and E). Similar results were observed with antibodies specific for Dsg1, Dsg2, and Dsc2/3 (data not shown). Furthermore, anti-plakoglobin antibodies labeled cell–cell contacts in both control and Sec3 knockdown cells, but the morphology of these contacts was abnormal when Sec3 expression was reduced (Figure 8C). In addition, plasma membrane labeling of desmoplakin and the Exocyst [as defined by Sec15 and Sec6(8A5) labeling] was substantially reduced in Sec3 knockdown cells (Figure 8C). In contrast, E-cadherin localization was largely unchanged when Sec3 expression was suppressed (Figure 8, D and E). On reexpression of Sec3 in these cells, desmoplakin and Sec15
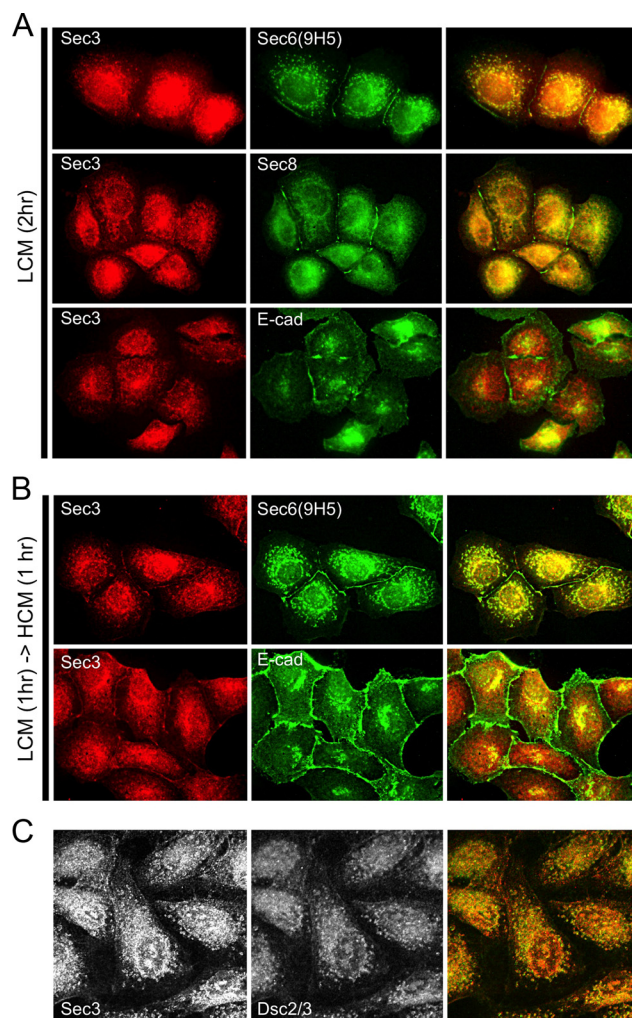

Figure 7. Plasma membrane recruitment of Sec3 is temporally distinct from that of Sec6 and Sec8. Low-density cultures of contact-naïve MDCK cells were seeded in LCM on collagen-coated coverslips and incubated for 2 h (A and C) or for 1 h, before shifting them to HCM for 1 h (B). (A) Cells were fixed and colabeled with anti-Sec3CT and anti-Sec6(9H5), anti-Sec8(8F12), or anti-E-cadherin antibodies. Note that within 2 h in LCM, E-cadherin, Sec6, and Sec8 were enriched at sites of cell–cell contact, but Sec3 was not recruited to plasma membranes under these conditions. (B) Cells were fixed and colabeled with anti-Sec3CT and anti-Sec6(9H5) or anti-E-cadherin antibodies. Under these culture conditions, Sec3 was observed to accumulate at sites of cell-cell contact. (C) Cells were fixed and colabeled with anti-Sec3CT and anti-Dsc2/3 antibodies. Note that cytoplasmic puncta of Sec3 colocalize with this desmosomal cadherin in contact-naïve cells.

were returned to the plasma membrane, and normal desmosomal morphology was restored (Figure 8C). Therefore, the absence of Sec3 seems to affect the morphology of desmosomes specifically and not that of adherens junctions.

Because the Exocyst has been implicated in vesicle tethering to target membranes, we investigated the possibility that Sec3 was required for trafficking of desmoglein-containing vesicles to the plasma membrane. The delivery of Dsg2 to the plasma membrane was assayed by biotin accessibility in a surface repopulation assay. Cells were suspended in trypsin to dissociate them and remove preexisting surface proteins, and then replated in LCM at confluent density. At various time points after transferring cells to HCM, Dsg2
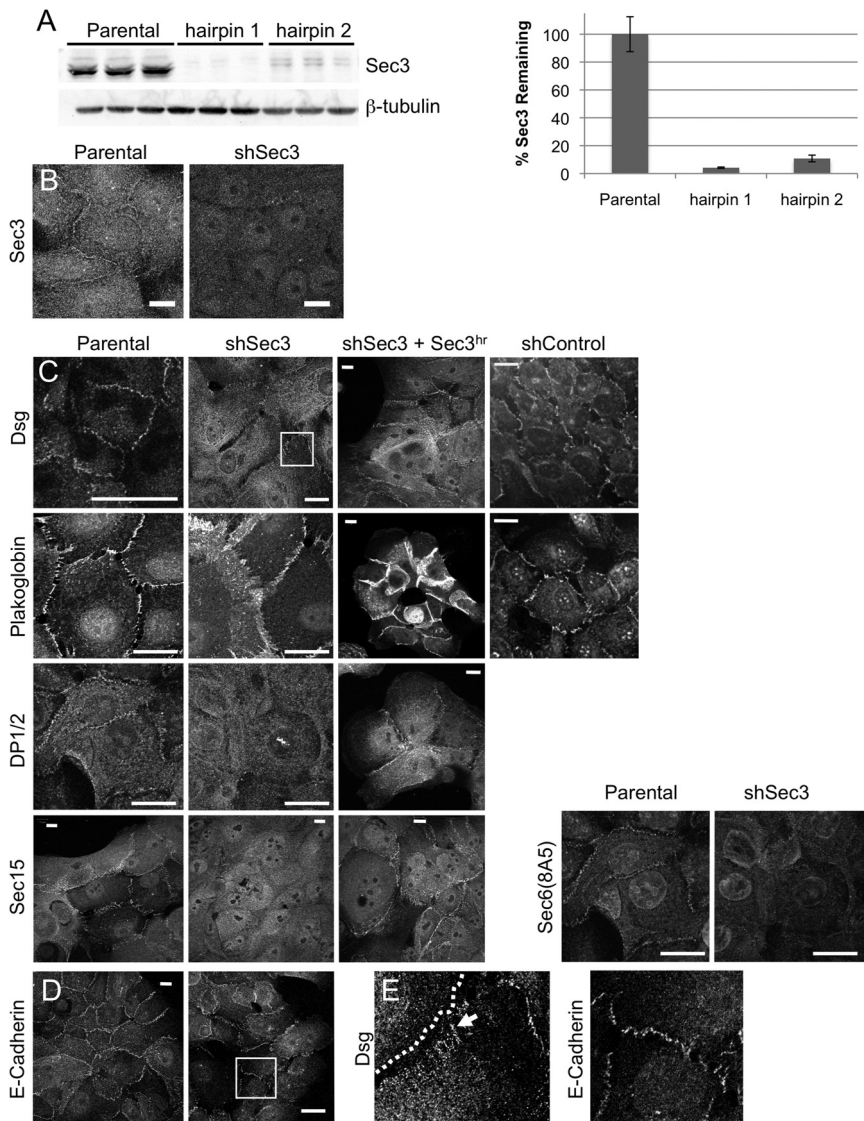
Figure 8. Sec3 is required for desmosome stability. (A) Lentiviruses producing hairpin 1 (nucleotides 1473-1493) or hairpin 2 (nucleotides 1244-1264), which are common to both splice variants of Sec3, were constructed. MCF-10A cells were transduced with these viruses and selected in 5 μg/ml puromycin. RIPA lysates, in triplicate, were resolved by SDS-PAGE and immunoblotted with anti-Sec3NT and anti-β-tubulin antibodies. Normalized Sec3 protein levels were determined and compared with that in parental MCF-10A cells. (B) Sec3 reduction was confirmed by immunofluorescence. Parental MCF-10A and shSec3 (hairpin 2) cells were labeled with anti-Sec3CT antibodies. Note the reduction of cytoplasmic and plasma membrane labeling in Sec3-knockdown cells. Bar, 10 μm. (C) Parental MCF-10A cells, shSec3 (hairpin 2) cells without or with ectopically expressed hairpin-resistant Sec3 (Sec3^{hr}), and MCF-10A cells stably expressing a control shRNA (shControl) were labeled with anti-pan-Dsg, anti-plakoglobin, anti-DP1/2, and anti-Sec15 antibodies. Bars, 20 μm. (D) Control and shSec3 cells were labeled with anti-E-cadherin antibodies. Bar, 20 μm. (E) Close-up of boxed regions in C and D. Note that Dsg is expressed diffusely at the surface of shSec3 cells and that its concentration at sites of intercellular contact is reduced. At such sites the protein is arranged in linear puncta (arrow) that run perpendicular to the cell boundary (dotted line). In contrast, E-cadherin expression and organization at sites of cell–cell contact seems normal in shSec3 cells.

expression at the plasma membrane was quantified by cell surface biotinylation, followed by streptavidin precipitation of biotinylated proteins. In control cells, Dsg2 gradually accumulated at the cell surface over a 72-h time course (Figure 9, A and B). Surprisingly, in Sec3-knockdown cells the rate of Dsg2 accumulation at the plasma membrane was increased relative to that in control cells, reaching steady state within 15–30 h of the calcium switch (Figure 9, A and B). However, the Dsg2 that was delivered to the plasma membrane did not seem to assemble into desmosomes (Figure 8, C and E). In contrast, E-cadherin transport was not altered after the suppression of Sec3 expression (Figure 8C). Therefore, loss of Sec3 expression is associated with changes in transport or incorporation of Dsg2 into desmosomes but not with trafficking of E-cadherin to developing adherens junctions.

To gain further insight into how a reduction in Sec3 expression affected desmosome structure and function, we quantified overall expression levels of several desmosome- and adherens junction-associated proteins in two independent clones of MCF-10A cells expressing hairpin 2. These clones exhibited an ~80–90% reduction of Sec3 expression (Figure 10A). In both clones, as well as in pools of cells

expressing either hairpin 1 or hairpin 2, the levels of all desmosomal cadherins examined were elevated relative to those in control cells (Figure 10B and Supplemental Figure S5). Dsg1expression was 1.4- and 3.2-fold higher in clones 1 and 2, respectively. Likewise, Dsg2 expression was 1.9- and 4.2-fold higher, and Dsc2/3 expression was 13- and 23-fold higher, in the Sec3 knockdown clones (Figure 10B). In addition, plakoglobin protein levels were increased, but desmoplakin expression was not substantially altered (Figure 10B). Expression of Sec3^{hr} in these cells partially reversed these effects, leading to a substantial reduction in Dsc2/3 expression and a more modest reduction in plakoglobin expression (Figure 10E). Adherens junction components, such as E-cadherin and α-catenin, were not consistently affected, indicating that effects of Sec3 knockdown were specific to desmosomes (Figure 10, C and D, and Supplemental Figure S5).

To determine whether observed changes in desmosome composition and morphology in Sec3-knockdown cells had functional consequences, we evaluated intercellular adhesion strength by hanging drop assay (Kim *et al.*, 2000; Huen *et al.*, 2002; Lorch *et al.*, 2004). After 20 h in suspension, both control and Sec3-knockdown cells had formed cellular aggregates of similar size and distribution (Figure 11). How-
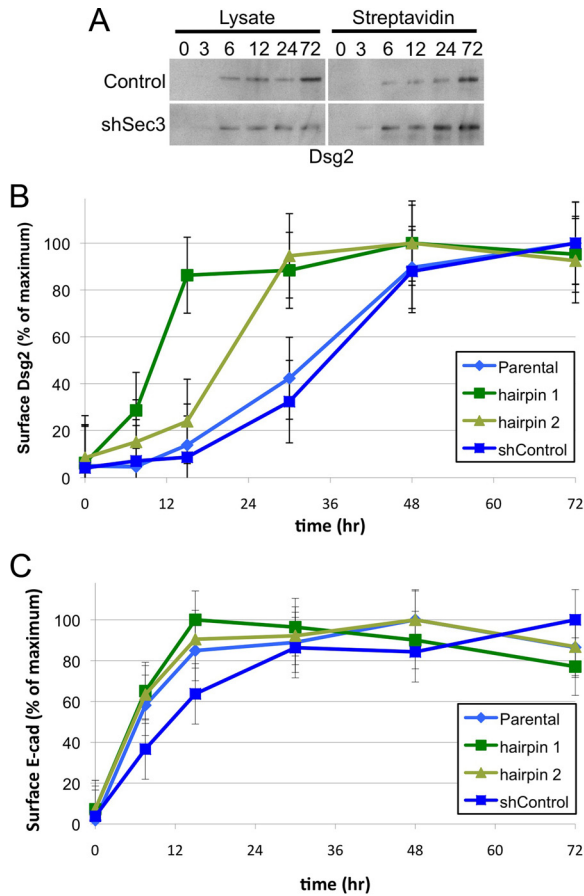
Figure 9. Sec3 is required for normal Dsg2 trafficking. A surface repopulation assay was performed in MCF-10A control and shSec3 cells, as described in *Materials and Methods*. At various time points after the calcium switch, surface proteins were biotinylated and precipitated with streptavidin agarose. (A) Samples of total cell lysate (10%) or streptavidin-agarose pull-downs (90%) were resolved by SDS-PAGE and immunoblotted with anti-Dsg2 antibody. (B) For each time point, normalized streptavidin-precipitate signals were compared with the maximum signal of cell surface Dsg2 for that cell type. Note that kinetics with which Dsg2 achieved a steady-state distribution at the plasma membrane were increased in shSec3 cells, relative to control cells. (C) Immunoblots were reprobed with anti-E-cadherin antibody and analyzed as in B. Note that kinetics with which E-cadherin achieved a steady-state distribution at the plasma membrane were not significantly altered in shSec3 cells, relative to control cells. Error bars are SEM (n = 9).

ever, application of an external force revealed a clear difference in relative adhesive strengths of the two cultures. Although the frequency of large aggregates (>50 cells) was reduced after trituration of either population, the extent to which each culture was affected was not the same. Whereas essentially all of the large cell aggregates were disrupted in Sec3-knockdown cultures, nearly 50% of such clusters were resistant to trituration in the control cultures (Figure 11). Consistent with the disruption of large aggregates, the number of single cells and doublets in Sec3-knockdown cultures was higher than that of larger aggregates (Figure 11). Collectively, these findings indicate that a Sec3-containing Exocyst localizes to desmosomes and is required for the assembly of functioning intercellular junctions between epithelial cells.
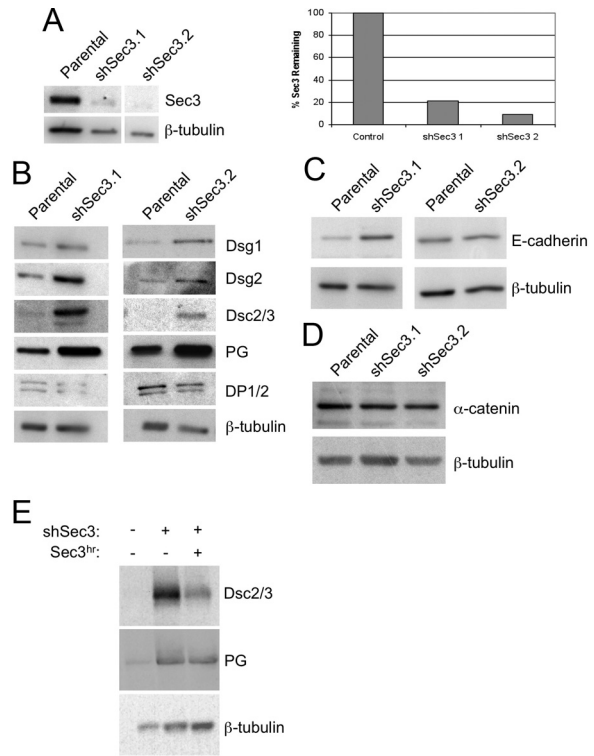

Figure 10. Suppression of Sec3 expression is associated with increases in overall expression levels of desmosomal cadherins and plakoglobin. (A) Two clonal populations of MCF-10A cells stably transduced with shSec3 (hairpin 2) were isolated and characterized. Sec3 and β-tubulin immunoblots were performed to determine the level of Sec3 reduction (values for each clone are normalized to control cultures). Note that clone 1 exhibited an almost 80% reduction of Sec3 and that clone 2 exhibited a >90% reduction. (B) Lysates of control MCF-10A or shSec3 clones 1 and 2 were immunoblotted with antibodies to desmosomal cadherins (Dsg1, Dsg2, and Dsc2/3), plakoglobin (PG), DP1/2, and β-tubulin. Dsg1 and 2, Dsc2/3, and plakoglobin protein levels were all increased in the Sec3 knockdown clones, relative to controls. DP1/2 protein levels did not change. (C and D) Immunoblots of two adherens junction-associated proteins, E-cadherin and α-catenin, showed no consistent changes in expression levels in the Sec3 knockdown clones. (E) Lysates of MCF-10A cells, shSec3 cells, or shSec3 cells transiently transfected with a plasmid encoding a hairpin-resistant variant (Sec3hr) were immunoblotted for Dsc2/3, PG and β-tubulin. Note that reexpression of Sec3 in cells partially reversed the elevation of desmosomal protein expression that accompanied Sec3 knockdown, as normalized levels of both Dsc2/3 and PG were lower in cells that received the Sec3 rescue construct.

DISCUSSION

In Mammalian Epithelial Cells, Sec3 Associates with a Subset of Exocyst Complexes That Are Enriched at Desmosomes and Centrosomes but Not AJCs

Immunolocalization studies of endogenous Exocyst complexes in mammalian epithelial cells have revealed that subunits of these complexes are present at the AJC (Sec6 and Sec8) (Grindstaff *et al.*, 1998; Charron *et al.*, 2000; Yeaman *et al.*, 2004), recycling endosomes (Sec8, Sec10, and Exo70) (Folsch *et al.*, 2003; Prigent *et al.*, 2003; Oztan *et al.*, 2007), and centrosomes/ciliary basal bodies (Sec6, Sec8, and Sec10) (Rogers *et al.*, 2004; Zuo *et al.*, 2009). Our study extends these findings to Sec3, antibodies to which labeled most of the same organelles, although Sec3 was notably absent from the AJC-associated Exocyst complex (see below). Findings from
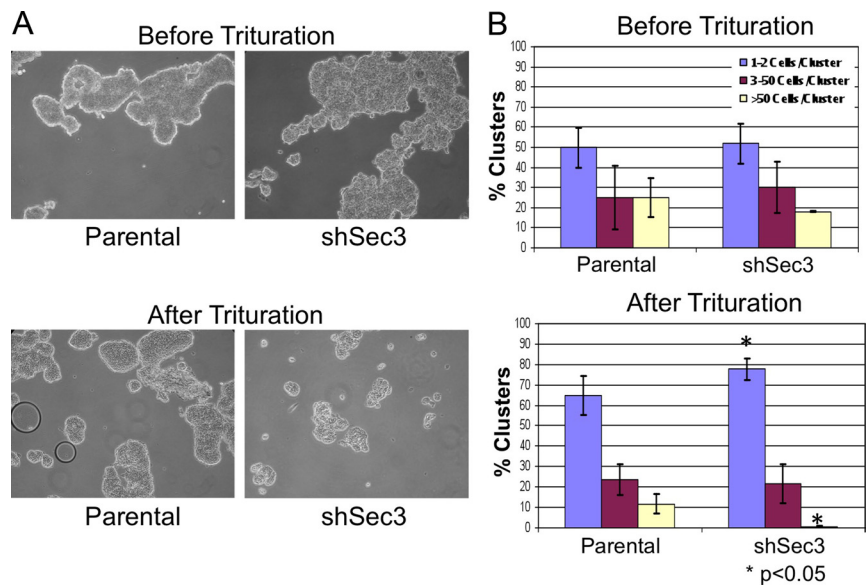
Figure 11. Sec3 is important for cell–cell adhesion. (A) MCF-10A parental and shSec3 cells before and after trituration. Representative images are shown. (B) Percentages of clusters with indicated numbers of cells were calculated, for control and shSec3 cells, before and after mechanical stress. Error bars represent standard deviations of the means of multiple determinations.

the current study have identified the desmosomes of epithelial cells as additional sites of Exocyst assembly and function; six subunits (Sec3, Sec6, Sec8, Sec15, Exo70, and Exo84) were detected there. In addition, the current study adds a subset of the same protein group (Sec3, Sec15, Exo70, and Exo84) to the Exocyst subunits that are known to be present at centrosomes. Collectively, these immunolabeling studies suggest that, in epithelial cells, desmosomes and centrosomes are likely to be the principle sites at which fully assembled Exocyst holocomplexes accumulate.

Our data also have revealed that the Sec6/8 complex assembled at the AJC is distinct from the Exocyst complex assembled at desmosomes. Polyclonal antibodies to Sec3, Sec10, Sec15, Exo70, and Exo84 did not label the AJC (Prigent *et al.*, 2003; Zuo *et al.*, 2009; this study). Although differential epitope accessibility has been offered as an explanation for the organelle-specific labeling patterns observed with several anti-Sec6 mAbs (Yeaman *et al.*, 2001), it is unlikely that epitope masking accounts for our inability to detect five distinct components (Sec3, Sec10, Sec15, Exo70, and Exo84) at the AJC, especially because polyclonal antibodies to each of these proteins were used in these studies. It is more likely that these subunits simply do not accumulate there. It thus remains unclear whether the AJC-associated Sec6/8 complex recruited to nascent E-cadherin–positive adhesion sites in advance of the assembly of Sec3-containing Exocyst complexes at desmosomes represents a by-product of the dynamic assembly and disassembly of Exocyst complexes in a variety of functional states or a truly distinct functional unit. It should be noted that a recent study identified, within yeast Sec6, conserved sequences that were capable of targeting the Exocyst to sites of polarized membrane trafficking, indicating that a functional Sec6/8 subcomplex could potentially target to the AJC in the absence of Sec3 (Songer and Munson, 2009).

Several lines of evidence support the existence of multiple Exocyst complexes or subcomplexes with distinct functions. First, antibodies to different subunits have been shown to differentially label subcellular compartments in many cell types (Yeaman *et al.*, 2001, 2004; Vik-Mo *et al.*, 2003; Beronja *et al.*, 2005; Mehta *et al.*, 2005) and, when applied in cell fractionation experiments, to identify discrete pools of Exocyst subunits (Guo *et al.*, 1999; Moskalenko *et al.*, 2003;

Beronja *et al.*, 2005). Second, distinct phenotypes have been associated with loss-of-function mutations in a variety of *Drosophila* Exocyst genes, and RNA interference (RNAi)-mediated silencing of different subunits in cell culture has likewise led to distinct phenotypes (Mehta *et al.*, 2005; Chien *et al.*, 2006; Zuo *et al.*, 2009). Third, mammalian genomes include two distinct Sec15-like genes, and as many as five Sec6-like genes; many or all of these encode proteins that are simultaneously expressed in the same cell and that interact with other Exocyst subunits, further increasing the potential diversity of Exocyst complexes in cells (Brymora *et al.*, 2001; Saito *et al.*, 2008; Spiczka and Yeaman, unpublished data). Therefore, the Sec3-containing Exocyst complex associated with desmosomes may represent only one member of a family of related tethering complexes that are expressed by epithelial cells to ensure targeted delivery of cargo-laden transport vesicles to the correct destination at the plasma membrane.

Sec3 Is Required for Desmosome Assembly

Using an RNAi approach, we investigated the role for the Sec3 protein in epithelial cells. Suppression of Sec3 expression resulted in a loss of Exocyst from desmosomes, consistent with conclusions from budding yeast that Sec3 directly binds plasma membrane phospholipids, and from this location coordinates the assembly of other subunits arriving on transport vesicles (Boyd *et al.*, 2004; Zhang *et al.*, 2008). The fact that the Exocyst was lost from desmosomes upon Sec3 knockdown suggests that transport vesicles were no longer targeted to these sites. However, this did not result in intracellular accumulation of the desmosomal cadherin Dsg2, which continued to be exocytosed in the absence of Sec3. This indicates that Dsg2-containing transport vesicles, once relieved of the spatial constraint to fuse only at desmosomes, were able to efficiently dock and fuse elsewhere on the plasma membrane. However, in Sec3 knockdown cells, the desmosomes had a distorted morphology, and hanging drop assays revealed that they were less adhesive than those in control cultures. Perhaps in response to these weakened junctions, cells increased the overall expression of many other desmosomal proteins. Importantly, effects of Sec3 knockdown were most acute at desmosomes, with AJCs not being noticeably impacted.

How might a Sec3-containing Exocyst complex function in desmosome assembly? Formation of this intercellular junction is a complex process, involving multiple phases of microtubule-dependent vesicular trafficking events that deliver membrane components (e.g., desmocollins, desmogleins, and plakoglobin) to the plasma membrane, in coordination with multiple phases of actin-dependent movement of plaque components (e.g., desmoplakin and plakophilin) (reviewed by Green and Simpson, 2007). Sec3, and by extension the Exocyst, could contribute to desmosome assembly in several different ways. As a putative vesicle tether, the Sec3-Exocyst might be required for the delivery of transport vesicles carrying desmosomal membrane components. Electron microscopy has showed that desmosome assembly involves two phases of vesicle delivery (Burdett and Sullivan, 2002). At early stages, small (60-nm) vesicles carrying mostly desmocollins were delivered to the plasma membrane in a nonpolarized manner. At later stages, larger (200-nm) vesicles carrying mostly desmogleins were targeted, in a polarized manner, to basal–lateral membranes at which desmosomes were forming. Live-cell imaging showed that vesicles carrying Dsg2-GFP explored different regions of the plasma membrane, before fusing with existing desmosomal puncta (Gloushankova *et al.*, 2003). It is possible that Sec3 is required for the second, polarized trafficking step, but not the first. Hence, the diffuse pattern of surface Dsg2 labeling observed in Sec3 knockdown cells might reflect vesicles that were delivered via a Sec3-independent, nonpolarized pathway.

An alternative possibility for Sec3 function at the desmosome is that it may organize microtubule tracks required for the efficient delivery of membrane components to desmosomes. This is consistent with previous suggestions of a role for the Exocyst in regulating microtubule dynamics (Vega and Hsu, 2001; Wang *et al.*, 2004; Liebl *et al.*, 2005). Furthermore, Sec3 was recently shown to bind IQGAP1, a Cdc42/Rac effector that interacts with the plus-end binding protein CLIP-170 to capture microtubules at the leading edge of migrating cells (Hart *et al.*, 1996; Kuroda *et al.*, 1996; Fukata *et al.*, 2002). Although a role for IQGAP1 at desmosomes has not been established, it is notable that CLIP-170 is associated with the plus ends of microtubules at desmosomes (Wacker *et al.*, 1992). It will be interesting to determine whether Sec3 contributes to the polarized delivery of cargo to developing desmosomes by facilitating microtubule organization.

Finally, it is possible that a desmosome-associated Exocyst complex helps to organize the actin cytoskeleton at these sites to facilitate the movement of plaque proteins. Careful live-cell imaging analysis of the dynamics with which desmoplakin-GFP was incorporated into forming desmosomes revealed that three phases of movement take place (Godsel *et al.*, 2005). After the rapid accumulation of one pool of desmoplakin at nascent cell–cell contact sites, a second pool was observed to accumulate in cortical puncta that were not membrane bound. Subsequently, these puncta moved in an actin-dependent manner, and with slower kinetics, to the membrane and then were incorporated into preexisting desmosomes. The organization of actin-based structures that facilitate the incorporation of desmoplakin into maturing desmosomes could be regulated by the Exocyst, which is known to regulate actin dynamics in other cell types through its interactions with the Arp2/3 complex (Zuo *et al.*, 2006).

In conclusion, this study shows that Sec3 targets Exocyst complexes to desmosomes in mammalian epithelial cells, and that these complexes are required for assembly of functional desmosomes. Moreover, we show that this complex is distinct from a previously characterized Sec6/8 complex at the AJC. Future studies will focus on elucidating the mechanisms by which these complexes regulate the development and maintenance of specialized membrane domains in polarized epithelial cells.

REFERENCES

Beronja, S., Laprise, P., Papoulas, O., Pellikka, M., Sisson, J., and Tepass, U. (2005). Essential function of *Drosophila* Sec6 in apical exocytosis of epithelial photoreceptor cells. J. Cell Biol. *169*, 635–646.

Blankenship, J. T., Fuller, M. T., and Zallen, J. A. (2007). The *Drosophila* homolog of the Exo84 exocyst subunit promotes apical epithelial identity. J. Cell Sci. *120*, 3099–3110.

Boyd, C., Hughes, T., Pypaert, M., and Novick, P. (2004). Vesicles carry most exocyst subunits to exocytic sites marked by the remaining two subunits, Sec3p and Exo70p. J. Cell Biol. *167*, 889–901.

Brymora, A., Valova, V. A., Larsen, M. R., Roufogalis, B. D., and Robinson, P. J. (2001). The brain exocyst complex interacts with RalA in a GTP-dependent manner: identification of a novel mammalian Sec3 gene and a second Sec15 gene. J. Biol. Chem. *276*, 29792–29797.

Burdett, I. D., and Sullivan, K. H. (2002). Desmosome assembly in MDCK cells: transport of precursors to the cell surface occurs by two phases of vesicular traffic and involves major changes in centrosome and Golgi location during a Ca(2+) shift. Exp. Cell Res. *276*, 296–309.

Cascone, I., Selimoglu, R., Ozdemir, C., Del Nery, E., Yeaman, C., White, M., and Camonis, J. (2008). Distinct roles of RalA and RalB in the progression of cytokinesis are supported by distinct RalGEFs. EMBO J. *27*, 2375–2387.

Charron, A. J., Nakamura, S., Bacallao, R., and Wandinger-Ness, A. (2000). Compromised cytoarchitecture and polarized trafficking in autosomal dominant polycystic kidney disease cells. J. Cell Biol. *149*, 111–124.

Chien, Y., *et al.* (2006). RalB GTPase-mediated activation of the IkappaB family kinase TBK1 couples innate immune signaling to tumor cell survival. Cell *127*, 157–170.

Cubelos, B., Gimenez, C., and Zafra, F. (2005). The glycine transporter GLYT1 interacts with Sec3, a component of the exocyst complex. Neuropharmacology *49*, 935–944.

Debnath, J., Muthuswamy, S. K., and Brugge, J. S. (2003). Morphogenesis and oncogenesis of MCF-10A mammary epithelial acini grown in three-dimensional basement membrane cultures. Methods *30*, 256–268.

Fielding, A. B., Schonteich, E., Matheson, J., Wilson, G., Yu, X., Hickson, G. R., Srivastava, S., Baldwin, S. A., Prekeris, R., and Gould, G. W. (2005). Rab11-FIP3 and FIP4 interact with Arf6 and the exocyst to control membrane traffic in cytokinesis. EMBO J. *24*, 3389–3399.

Finger, F. P., Hughes, T. E., and Novick, P. (1998). Sec3p is a spatial landmark for polarized secretion in budding yeast. Cell *92*, 559–571.

Finger, F. P., and Novick, P. (1997). Sec3p is involved in secretion and morphogenesis in *Saccharomyces cerevisiae*. Mol. Biol. Cell *8*, 647–662.

Flory, M. R., Moser, M. J., Monnat, R. J., Jr., and Davis, T. N. (2000). Identification of a human centrosomal calmodulin-binding protein that shares homology with pericentrin. Proc. Natl. Acad. Sci. USA *97*, 5919–5923.

Folsch, H., Pypaert, M., Maday, S., Pelletier, L., and Mellman, I. (2003). The AP-1A and AP-1B clathrin adaptor complexes define biochemically and functionally distinct membrane domains. J. Cell Biol. *163*, 351–362.

Fukata, M., Watanabe, T., Noritake, J., Nakagawa, M., Yamaga, M., Kuroda, S., Matsuura, Y., Iwamatsu, A., Perez, F., and Kaibuchi, K. (2002). Rac1 and Cdc42 capture microtubules through IQGAP1 and CLIP-170. Cell *109*, 873–885.

Gaudry, C. A., Palka, H. L., Dusek, R. L., Huen, A. C., Khandekar, M. J., Hudson, L. G., and Green, K. J. (2001). Tyrosine-phosphorylated plakoglobin is associated with desmogleins but not desmoplakin after epidermal growth factor receptor activation. J. Biol. Chem. *276*, 24871–24880.

Getsios, S., Amargo, E. V., Dusek, R. L., Ishii, K., Sheu, L., Godsel, L. M., and Green, K. J. (2004). Coordinated expression of desmoglein 1 and desmocollin 1 regulates intercellular adhesion. Differentiation 72, 419–433.

Gloushankova, N. A., Wakatsuki, T., Troyanovsky, R. B., Elson, E., and Troyanovsky, S. M. (2003). Continual assembly of desmosomes within stable intercellular contacts of epithelial A-431 cells. Cell Tissue Res. 314, 399–410.

Godsel, L. M., et al. (2005). Desmoplakin assembly dynamics in four dimensions: multiple phases differentially regulated by intermediate filaments and actin. J. Cell Biol. 171, 1045–1059.

Green, K. J., and Simpson, C. L. (2007). Desmosomes: new perspectives on a classic. J. Invest. Dermatol. 127, 2499–2515.

Grindstaff, K. K., Yeaman, C., Anandasabapathy, N., Hsu, S. C., Rodriguez-Boulan, E., Scheller, R. H., and Nelson, W. J. (1998). Sec6/8 complex is recruited to cell-cell contacts and specifies transport vesicle delivery to the basal-lateral membrane in epithelial cells. Cell 93, 731–740.

Gromley, A., Yeaman, C., Rosa, J., Redick, S., Chen, C. T., Mirabelle, S., Guha, M., Sillibourne, J., and Doxsey, S. J. (2005). Centriolin anchoring of exocyst and SNARE complexes at the midbody is required for secretory-vesicle-mediated abscission. Cell 123, 75–87.

Guo, W., Roth, D., Walch-Solimena, C., and Novick, P. (1999). The exocyst is an effector for Sec4p, targeting secretory vesicles to sites of exocytosis. EMBO J. 18, 1071–1080.

Guo, W., Tamanoi, F., and Novick, P. (2001). Spatial regulation of the exocyst complex by Rho1 GTPase. Nat. Cell Biol. 3, 353–360.

Hala, M., et al. (2008). An exocyst complex functions in plant cell growth in Arabidopsis and tobacco. Plant Cell 20, 1330–1345.

Hart, M. J., Callow, M. G., Souza, B., and Polakis, P. (1996). IQGAP1, a calmodulin-binding protein with a rasGAP-related domain, is a potential effector for cdc42Hs. EMBO J. 15, 2997–3005.

Hazuka, C. D., Foletti, D. L., Hsu, S. C., Kee, Y., Hopf, F. W., and Scheller, R. H. (1999). The sec6/8 complex is located at neurite outgrowth and axonal synapse-assembly domains. J. Neurosci. 19, 1324–1334.

He, B., Xi, F., Zhang, X., Zhang, J., and Guo, W. (2007). Exo70 interacts with phospholipids and mediates the targeting of the exocyst to the plasma membrane. EMBO J. 26, 4053–4065.

Hinck, L., Nelson, W. J., and Papkoff, J. (1994). Wnt-1 modulates cell-cell adhesion in mammalian cells by stabilizing beta-catenin binding to the cell adhesion protein cadherin. J. Cell Biol. 124, 729–741.

Hsu, S. C., Ting, A. E., Hazuka, C. D., Davanger, S., Kenny, J. W., Kee, Y., and Scheller, R. H. (1996). The mammalian brain rsec6/8 complex. Neuron 17, 1209–1219.

Huen, A. C., et al. (2002). Intermediate filament-membrane attachments function synergistically with actin-dependent contacts to regulate intercellular adhesive strength. J. Cell Biol. 159, 1005–1017.

Kee, Y., Yoo, J. S., Hazuka, C. D., Peterson, K. E., Hsu, S. C., and Scheller, R. H. (1997). Subunit structure of the mammalian exocyst complex. Proc. Natl. Acad. Sci. USA 94, 14438–14443.

Kim, J. B., Islam, S., Kim, Y. J., Prudoff, R. S., Sass, K. M., Wheelock, M. J., and Johnson, K. R. (2000). N-Cadherin extracellular repeat 4 mediates epithelial to mesenchymal transition and increased motility. J. Cell Biol. 151, 1193–1206.

Kizhatil, K., and Bennett, V. (2004). Lateral membrane biogenesis in human bronchial epithelial cells requires 190-kDa ankyrin-G. J. Biol. Chem. 279, 16706–16714.

Klessner, J. L., Desai, B. V., Amargo, E. V., Getsios, S., and Green, K. J. (2009). EGFR and ADAMs cooperate to regulate shedding and endocytic trafficking of the desmosomal cadherin desmoglein 2. Mol. Biol. Cell 20, 328–337.

Kuroda, S., Fukata, M., Kobayashi, K., Nakafuku, M., Nomura, N., Iwamatsu, A., and Kaibuchi, K. (1996). Identification of IQGAP as a putative target for the small GTPases, Cdc42 and Rac1. J. Biol. Chem. 271, 23363–23367.

Langevin, J., Morgan, M. J., Sibarita, J. B., Aresta, S., Murthy, M., Schwarz, T., Camonis, J., and Bellaiche, Y. (2005). Drosophila exocyst components Sec5, Sec6, and Sec15 regulate DE-Cadherin trafficking from recycling endosomes to the plasma membrane. Dev. Cell 9, 365–376.

Lavy, M., Bloch, D., Hazak, O., Gutman, I., Poraty, L., Sorek, N., Sternberg, H., and Yalovsky, S. (2007). A Novel ROP/RAC effector links cell polarity, root-meristem maintenance, and vesicle trafficking. Curr. Biol. 17, 947–952.

Liebl, F. L., Chen, K., Karr, J., Sheng, Q., and Featherstone, D. E. (2005). Increased synaptic microtubules and altered synapse development in Drosophila sec8 mutants. BMC Biol. 3, 27.

Lipschutz, J. H., Guo, W., O'Brien, L. E., Nguyen, Y. H., Novick, P., and Mostov, K. E. (2000). Exocyst is involved in cystogenesis and tubulogenesis

and acts by modulating synthesis and delivery of basolateral plasma membrane and secretory proteins. Mol. Biol. Cell 11, 4259–4275.

Lipschutz, J. H., Lingappa, V. R., and Mostov, K. E. (2003). The exocyst affects protein synthesis by acting on the translocation machinery of the endoplasmic reticulum. J. Biol. Chem. 278, 20954–20960.

Liu, J., Zuo, X., Yue, P., and Guo, W. (2007). Phosphatidylinositol 4,5-bisphosphate mediates the targeting of the exocyst to the plasma membrane for exocytosis in mammalian cells. Mol. Biol. Cell 18, 4483–4492.

Lorch, J. H., Klessner, J., Park, J. K., Getsios, S., Wu, Y. L., Stack, M. S., and Green, K. J. (2004). Epidermal growth factor receptor inhibition promotes desmosome assembly and strengthens intercellular adhesion in squamous cell carcinoma cells. J. Biol. Chem. 279, 37191–37200.

Malhotra, V., Serafini, T., Orci, L., Shepherd, J. C., and Rothman, J. E. (1989). Purification of a novel class of coated vesicles mediating biosynthetic protein transport through the Golgi stack. Cell 58, 329–336.

Marrs, J. A., Napolitano, E. W., Murphy-Erdosh, C., Mays, R. W., Reichardt, L. F., and Nelson, W. J. (1993). Distinguishing roles of the membrane-cytoskeleton and cadherin mediated cell-cell adhesion in generating different Na+,K(+)-ATPase distributions in polarized epithelia. J. Cell Biol. 123, 149–164.

Matern, H. T., Yeaman, C., Nelson, W. J., and Scheller, R. H. (2001). The Sec6/8 complex in mammalian cells: characterization of mammalian Sec3, subunit interactions, and expression of subunits in polarized cells. Proc. Natl. Acad. Sci. USA 98, 9648–9653.

Mehta, S. Q., et al. (2005). Mutations in Drosophila sec15 reveal a function in neuronal targeting for a subset of exocyst components. Neuron 46, 219–232.

Moskalenko, S., Tong, C., Rosse, C., Mirey, G., Formstecher, E., Daviet, L., Camonis, J., and White, M. A. (2003). Ral GTPases regulate exocyst assembly through dual subunit interactions. J. Biol. Chem. 278, 51743–51748.

Overgaard, C. E., Sanzone, K. M., Spiczka, K. S., Sheff, D. R., Sandra, A., and Yeaman, C. (2009). Deciliation is associated with dramatic remodeling of epithelial cell junctions and surface domains. Mol. Biol. Cell 20, 102–113.

Oztan, A., Silvis, M., Weisz, O. A., Bradbury, N. A., Hsu, S. C., Goldenring, J. R., Yeaman, C., and Apodaca, G. (2007). Exocyst requirement for endocytic traffic directed toward the apical and basolateral poles of polarized MDCK cells. Mol. Biol. Cell 18, 3978–3992.

Park, T. J., Mitchell, B. J., Abitua, P. B., Kintner, C., and Wallingford, J. B. (2008). Dishevelled controls apical docking and planar polarization of basal bodies in ciliated epithelial cells. Nat. Genet. 40, 871–879.

Prigent, M., Dubois, T., Raposo, G., Derrien, V., Tenza, D., Rosse, C., Camonis, J., and Chavrier, P. (2003). ARF6 controls post-endocytic recycling through its downstream exocyst complex effector. J. Cell Biol. 163, 1111–1121.

Rogers, K. K., Wilson, P. D., Snyder, R. W., Zhang, X., Guo, W., Burrow, C. R., and Lipschutz, J. H. (2004). The exocyst localizes to the primary cilium in MDCK cells. Biochem. Biophys. Res. Commun. 319, 138–143.

Rosse, C., Hatzoglou, A., Parrini, M. C., White, M. A., Chavrier, P., and Camonis, J. (2006). RalB mobilizes the exocyst to drive cell migration. Mol. Cell. Biol. 26, 727–734.

Saito, T., Shibasaki, T., and Seino, S. (2008). Involvement of Exoc3l, a protein structurally related to the exocyst subunit Sec6, in insulin secretion. Biomed. Res. 29, 85–91.

Sakurai-Yageta, M., Recchi, C., Le Dez, G., Sibarita, J. B., Daviet, L., Camonis, J., D'Souza-Schorey, C., and Chavrier, P. (2008). The interaction of IQGAP1 with the exocyst complex is required for tumor cell invasion downstream of Cdc42 and RhoA. J. Cell Biol. 181, 985–998.

Shin, D. M., Zhao, X. S., Zeng, W., Mozhayeva, M., and Muallem, S. (2000). The mammalian Sec6/8 complex interacts with Ca(2+) signaling complexes and regulates their activity. J. Cell Biol. 150, 1101–1112.

Simons, M., Saffrich, R., Reiser, J., and Mundel, P. (1999). Directed membrane transport is involved in process formation in cultured podocytes. J. Am. Soc. Nephrol. 10, 1633–1639.

Songer, J. A., and Munson, M. (2009). Sec6p anchors the assembled exocyst complex at sites of secretion. Mol. Biol. Cell 20, 973–982.

Spiczka, K. S., and Yeaman, C. (2008). Ral-regulated interaction between Sec5 and paxillin targets Exocyst to focal complexes during cell migration. J. Cell Sci. 121, 2880–2891.

Stewart, D. B., and Nelson, W. J. (1997). Identification of four distinct pools of catenins in mammalian cells and transformation-dependent changes in catenin distributions among these pools. J. Biol. Chem. 272, 29652–29662.

Tait, L., Soule, H. D., and Russo, J. (1990). Ultrastructural and immunocytochemical characterization of an immortalized human breast epithelial cell line, MCF-10. Cancer Res. 50, 6087–6094.

TerBush, D. R., Maurice, T., Roth, D., and Novick, P. (1996). The Exocyst is a multiprotein complex required for exocytosis in *Saccharomyces cerevisiae*. EMBO J. *15*, 6483–6494.

TerBush, D. R., and Novick, P. (1995). Sec6, Sec8, and Sec15 are components of a multisubunit complex which localizes to small bud tips in *Saccharomyces cerevisiae*. J. Cell Biol. *130*, 299–312.

Vega, I. E., and Hsu, S. C. (2001). The exocyst complex associates with microtubules to mediate vesicle targeting and neurite outgrowth. J. Neurosci. *21*, 3839–3848.

Vik-Mo, E. O., Oltedal, L., Hoivik, E. A., Kleivdal, H., Eidet, J., and Davanger, S. (2003). Sec6 is localized to the plasma membrane of mature synaptic terminals and is transported with secretogranin II-containing vesicles. Neuroscience *119*, 73–85.

Wacker, I. U., Rickard, J. E., De Mey, J. R., and Kreis, T. E. (1992). Accumulation of a microtubule-binding protein, pp170, at desmosomal plaques. J. Cell Biol. *117*, 813–824.

Wahl, J. K., 3rd. (2002). Generation of monoclonal antibodies specific for desmoglein family members. Hybrid Hybridomics *21*, 37–44.

Wahl, J. K., Sacco, P. A., McGranahan-Sadler, T. M., Sauppe, L. M., Wheelock, M. J., and Johnson, K. R. (1996). Plakoglobin domains that define its association with the desmosomal cadherins and the classical cadherins: identification of unique and shared domains. J. Cell Sci. *109*, 1143–1154.

Wang, S., Liu, Y., Adamson, C. L., Valdez, G., Guo, W., and Hsu, S. C. (2004). The mammalian exocyst, a complex required for exocytosis, inhibits tubulin polymerization. J. Biol. Chem. *279*, 35958–35966.

Wiederkehr, A., De Craene, J. O., Ferro-Novick, S., and Novick, P. (2004). Functional specialization within a vesicle tethering complex: bypass of a subset of exocyst deletion mutants by Sec1p or Sec4p. J. Cell Biol. *167*, 875–887.

Wollner, D. A., Krzeminski, K. A., and Nelson, W. J. (1992). Remodeling the cell surface distribution of membrane proteins during the development of epithelial cell polarity. J. Cell Biol. *116*, 889–899.

Yeaman, C. (2003). Ultracentrifugation-based approaches to study regulation of Sec6/8 (exocyst) complex function during development of epithelial cell polarity. Methods *30*, 198–206.

Yeaman, C., Grindstaff, K. K., and Nelson, W. J. (2004). Mechanism of recruiting Sec6/8 (exocyst) complex to the apical junctional complex during polarization of epithelial cells. J. Cell Sci. *117*, 559–570.

Yeaman, C., Grindstaff, K. K., Wright, J. R., and Nelson, W. J. (2001). Sec6/8 complexes on trans-Golgi network and plasma membrane regulate late stages of exocytosis in mammalian cells. J. Cell Biol. *155*, 593–604.

Zhang, X., Bi, E., Novick, P., Du, L., Kozminski, K. G., Lipschutz, J. H., and Guo, W. (2001). Cdc42 interacts with the exocyst and regulates polarized secretion. J. Biol. Chem. *276*, 46745–46750.

Zhang, X., Orlando, K., He, B., Xi, F., Zhang, J., Zajac, A., and Guo, W. (2008). Membrane association and functional regulation of Sec3 by phospholipids and Cdc42. J. Cell Biol. *180*, 145–158.

Zuo, X., Guo, W., and Lipschutz, J. H. (2009). The exocyst protein Sec10 is necessary for primary ciliogenesis and cystogenesis in vitro. Mol. Biol. Cell *20*, 2522–2529.

Zuo, X., Zhang, J., Zhang, Y., Hsu, S. C., Zhou, D., and Guo, W. (2006). Exo70 interacts with the Arp2/3 complex and regulates cell migration. Nat. Cell Biol. *8*, 1383–1388.